Cooling efficiency and losses in electrocaloric materials

N. Zeggai, B. Dkhil, M. Lobue, M. Almanza

Cooling efficiency and losses in electrocaloric materials

N. Zeggai, M. LoBue, and M. Almanza
Université Paris-Saclay, ENS Paris-Saclay, CNRS, SATIE, 91190, Gif-sur-Yvette, France

B. Dkhil
Université Paris-Saclay, CentraleSupelec, CNRS, SPMS, 91190, Gif-sur-Yvette, France
(Dated: March 6, 2023)

A new figure of merit for assessing the cooling efficiency of electrocaloric (EC) materials is defined, where the caloric properties are taken into account jointly with the material's losses. Using a specifically developed measurement setup, based on flexible thermistances, the caloric effect and the losses are directly measured on P(VDF-TrFE-CFE) electrocaloric polymer films. The data are used, jointly with the new figure of merit, to extrapolate the cooling efficiency to be expected, under actual working conditions, from the studied EC material. Dielectric losses emerge as a major limiting factor for achieving the needed cooling performance. This finding shows that, beside the research for huge caloric response, material loss reduction has to be considered a key objective for researching an optimal EC refrigerant for cooling applications. Eventually, some strategies towards loss reduction are outlined.

The demand for cooling is experiencing dramatic growth, and today accounts for a significant share of global electricity consumption [1, 2]. Nowadays, this need is mainly met by vapour-compression refrigerators. Unfortunately, most of the available gaseous refrigerants are far to be eco-friendly. Interestingly, solid state refrigeration systems based on electrocaloric (EC) materials has emerged as a promising route for cooling [3–7]. Among these materials, the lead-free P(VDF-TrFE-CFE) terpolymer (terPo) ferroelectric has been considered as one of the most promising refrigerants, and deployed in some new cooling devices because of it strong electrocaloric response [4, 8].

EC effect is the reversible thermal change of a dipolar solid when the electric field is applied and withdrawn. Like other caloric effects, it is defined through two key quantities measured under a field variation: the isothermal entropy change Δs, and the adiabatic temperature change ΔT_{ad}. The EC effect characterization has often been performed by indirect measurements, relying on the use of the Maxwell relations [3, 9]. However, these relations are verified at equilibrium, where thermodynamic potentials of the system are convex [10], and their use in presence of hysteresis can give unreliable results, as put in [11], and discussed in [12] for the case of magnetocaloric materials. On the other hand, direct methods are based either on calorimetric measurements [13] where the heat δQ (i.e $T\Delta s$) is measured along an isotherm transformation, or on thermometric ones where ΔT_{ad} is measured along an adiabatic transformation [4, 8].

Unfortunately, carrying out calorimetric measurements close to the operating point can be rather challenging. For instance, due to the typical response times of thermal flux sensors, calorimetry may require measurements lasting several seconds, which can be far too long compared with the operating conditions of EC devices, (1 Hz[14, 15]). Besides, using standard sensors (viz. thermocouples, thermistances) to measure temperature of terPo films with thickness below 50 μm, can be difficult as the sensor mass must be reduced to prevent interfering with the EC effect. Contactless methods, as infrared measurements, require a high and well known emissivity, and strongly depend on the surface quality of the electrodes (i.e. deposition conditions), and on their type (i.e. carbon, gold, aluminium) [16].

Appropriate measurement set-ups enabling a proper assessment of the key features of EC materials, especially in working conditions, are therefore crucially needed.

Moreover, beside maximizing ΔT_{ad}, and $T\Delta s$, and optimizing efficiency through device design, reducing material losses is an objective of the utmost relevance in order to achieve EC refrigerants able to respond to the needs of a new generation of solid-state based cooling devices.Nevertheless, while maximizing material response [17], and getting an optimal reversible heat exchange [18],have been often addressed, with the notable exception of some approaches taking into account material hysteresis [19, 20], EC dielectric losses have been hitherto pretty neglected. Thus, there is an urgent need to define a meaningful and suitable electrocaloric figure of merit for cooling applications taking into account jointly caloric performance, and losses.

In this letter, a new figure of merit for the cooling efficiency is introduced. To show its usefulness for assessing the cooling performance of a material under working conditions, a fast ($\approx$ 1 ms) and sensitive (10 mK) temperature measurement setup is developed, and used to characterize a thin and flexible terPo ferroelectric film. Working frequencies, and applied fields are studied according to the typical existing refrigeration cycles, and the results are compared with those obtained under the excitation conditions commonly used for laboratory characterization (i.e. uni-polar sinusoidal waveform). As a result, we show that the caloric response and the losses are strongly affected by the voltage profile, and the frequency. Eventually, the terPo maximum efficiency estimated from our measurements is compared to the reported cooling efficiencies of actual devices [4, 8] showing a good agreement with data from the literature.

The approach presented here hinges on the study of the entropy production over a cyclical transformation. Considering the total entropy change along a cycle, as the sum of the reversibly exchanged Δs_e and the irreversibly produced Δs_i entropy changes, the efficiency of a cooling cycle working between two ideal equilibrium reservoirs at temperatures T_h, and

T_c, with $T_h > T_c$, can be written as follows [21]:

$$\eta = \frac{\eta_C}{1+\Delta s_i T_h \eta_C / Q_c} \tag{1}$$

with η_C the Carnot efficiency of a refrigerator working between T_c and T_h , and Q_c the heat exchanged with the cold reservoir. Let us now consider a cooling cycle where all the irreversible processes are negligible (film actuation, the thermal exchanges with the reservoirs), except the ones taking place within the refrigerant material itself. This is equivalent to consider a reversible work source, and two reversible heat sources acting on an irreversible active material. In this situation, all the energy losses $\mathscr{E}_{loss}$ produced within the EC material must be expelled, in the form of heat, towards the hot end, so that $\Delta s_i = \mathscr{E}_{loss}/T_h$. The working point of the refrigerator is set by the temperature difference between the reservoirs, $\Delta T_{res} = T_h - T_c$, the maximum material adiabatic temperature change ΔT_{ad}, the material isothermal entropy change Δs, and the two electric fields among which the cycle takes place, E_{max}, and 0. In order to approach a Carnot cycle (i.e. two isotherms, and two adiabats as in the dashed rectangular cycle shown in Fig. 1), the material temperature is kept constant along the isotherms by the caloric effect driven by the field change. This entails a trade-off between the ECE fraction used to isothermally change the entropy (i.e. the horizontal width of the isotherms in Fig. 1), and the one used for the adiabatic temperature change (i.e. the height of the cycle in Fig. 1). We shall describe this trade-off, through the parameter: $x = 1 - \Delta T_{res}/\Delta T_{ad}$. As $Q_c = x T_c \Delta s$, the relative efficiency writes,

$$\eta_r(x) = \frac{\eta}{\eta_C} = \left(1 + \frac{\mathscr{E}_{loss}}{x T_c \Delta s} \frac{T_c}{(1-x)\Delta T_{ad}}\right)^{-1}, \tag{2}$$

maximizing $\eta_r(x)$ with respect to x for a fixed ΔT_{ad} gives,

$$\eta_{max} = \frac{1}{1+4R}, \tag{3}$$

where we introduced the loss factor $R = \mathscr{E}_{loss}/(\Delta s \Delta T_{ad})$. The maximum relative efficiency η_{max}, as shown in the right panel of Fig. 1, takes place at $x = 0.5$, namely when $\Delta T_{res} = \Delta T_{ad}/2$. This maximum depends only on the loss factor R.

As a result, maximizing the relative efficiency requires the material loss factor minimization, meaning that ΔT_{ad} must be increased, and the material losses $\mathscr{E}_{loss}$ must be reduced. Therefore, searching the best EC refrigerant focusing exclusively on the adiabatic temperature change response, and neglecting material losses, misses a key point of the overall optimization of a cooling device.

In what follows we shall use this approach, based on the loss factor R, to study the electrocaloric features including the losses of a terpolymer ferroelectric material that has been used, as refrigerant, in some recently reported EC cooling devices [4, 8].

A TerPo (Piezotech Arkema, P(VDF-TrFE-CFE) 64.6/26.2/9.2 mol %) was dissolved at 10 wt% in MEK (methyl ethyl ketone) purchased from Sigma Aldrich. The solution has been stirred with a magnetic bar for 3 hours at 50°C. Afterwards it has been deposited by tape casting on glass substrate, and dried for 16 h, at 60 °C. The prepared films with 27 ± 0.5 μm thickness were collected using a few drops of distilled water. Finally, the freestanding films have been annealed for 24 h at 125°C. To form a capacitor structure, 40 nm thick Au electrodes were sputtered on each side of the film using evaporation technique. The capacitor is supplied by a high-voltage amplifier (Matsusada AMP-10B10), and the current and the voltage are simultaneously measured in order to obtain the polarization-electric field ($P-E$) hysteresis loops. The temperature of the electrocaloric material has been determined by measuring the resistance of a flexible and thin thermistor in contact with the film active part. The thermistor consists of a 8 μm thick polypropylene (PP) film, metallized with a 8 nm aluminum layer (Goodfellow, PP30-MZ-000180). Part of the metallization was removed to form a serpentine on the area of measurement using a fiber laser (Trotec, speedy 360 flexx), correctly configured to remove only the metallization without damaging the PP film. The resistance of the flexible thermistor (i.e. ≈ 1 kΩ) is measured, every 50 ms, with a 4-point probe using a digital multimeter (Keysight 34465A) reaching a sensitivity of 0.025°C. The thermistor surface, 8×8 mm^2, is smaller than that of the EC film, 10×10 mm^2. After calibration, the thermistor shows an excellent linear dependence between resistance and temperature in the interval between -10°C and 60°C, with a temperature coefficient resistance of 0.2299%. Besides, the thermistor resistance is unaffected by the ECM electrostriction because the associated deformation is isotropic in the film plane.

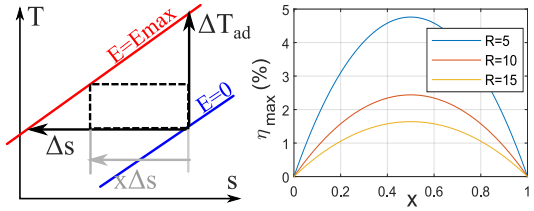

FIG. 1. In the left: The Carnot like cycles in between $E_{min} = 0$ and E_{max} and parameterized with x; the blue and the red lines show $s(T, E_{max})$ and $s(T, 0)$. In the right: the relative efficiency plotted against x for different loss factors R.

Due to its flexibility and to the adhesion forces, the thermistor spreads over the electrocaloric film. The quality of the thermal contact between film and thermistor is the key to reduce the sensor time response. To get insights into the reliability of the measurements, a simulation to assess the effect of undesired air gaps has been performed using a 1D numerical model of a multilayer, as depicted in the inset of Fig. 2. A variable air-gap between thermistor and electrocaloric film, as well as 2 mm air columns above, and below the bilayer are taken into account. For various air-gap thicknesses, Fig. 2 shows the time t dependence of the temperature of the film, and of the thermistor following a 1 K temperature jump within the EC film taking place at $t = 0$, and air-gap thickness from

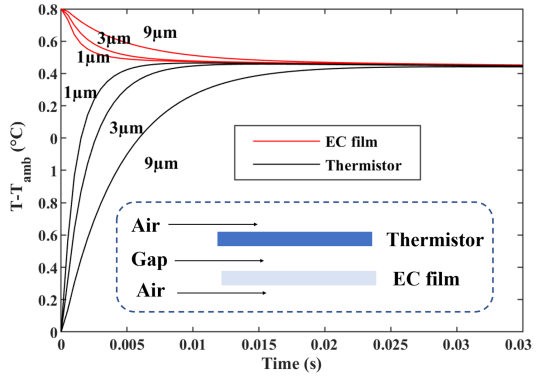

FIG. 2. 1D Numerical modeling of the time evolution of the thermistor, and the ECM film temperature (relative to the ambient temperature, T_{amb}), following a 1 K step-like temperature increasing within the caloric film. The value of the thickness of air gap simulated are indicated next to the corresponding curve.

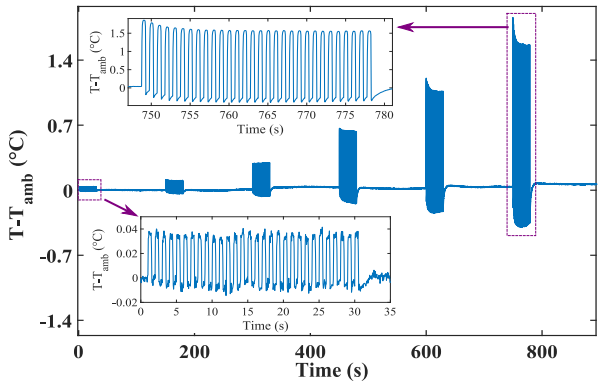

FIG. 3. Temperature of the ECM with an unipolar square profile with 10, 20, 30, 40, 50 and 60 $V/\mu m$ amplitude, and with 120 s stop between each field value. The insets show zoom in for 10 and 60 $V/\mu m$.

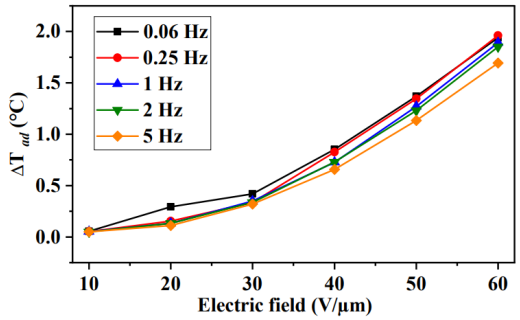

FIG. 4. Adiabatic temperature change as a function of the field, and for different frequencies

1 μm, up to 9 μm (a pretty high upper limit considering the thermistor thickness). Over a short period of time after the temperature step (i.e. $t \leq 0.01$ s), the film exchange heat primarily with the thermistor. Afterwards, at about $t \gtrsim 0.01$ s, the film and the thermistor reach the same temperature, and they slowly exchange heat with the surrounding air. The PP thermal load is known because the capacitor film properties are well controlled, the main uncertainty coming from a $\pm 5\%$ error at worst on the thickness. Taking into account the thermistor thermal load, the ratio between the thermistor and the film temperatures is estimated to be 1.19.

The EC material has been characterized under a square unipolar voltage waveform (0 to E_{max}). The unipolar field excitation provides a caloric response similar to the bipolar one (-E_{max} to E_{max}) with a loss reduction. In addition, the square waveform provides an excitation like the one used in actual cooling devices where two adiabats alternate with two constant field transformations (i.e. a Brayton cycle). The two voltage steps within the square waveform can be considered as adiabatic field changes. The ΔT_{ad} plotted in Fig.3 has been measured using the thermistor sensor on the terPo film when the field is removed. It shows an increase from 0.03°C to 2°C when the electric field varies from 10 Vμm^{-1} to 60 Vμm^{-1}. These values are in agreement with the ones reported in the literature [4, 8]. Fig. 4 and 5 show ΔT_{ad}, and $\mathscr{E}_{loss}$ respectively, measured in steady state under different frequencies and field amplitudes. The field increasing entails a significant raise of both ΔT_{ad} and $\mathscr{E}_{loss}$. Working at low frequency with the square profile slightly increases the adiabatic temperature response, as well as the losses. For comparison, losses measured under a sinusoidal waveform at the maximum field amplitude are plotted in Fig. 5. The sinusoidal waveform is the standard excitation used for material characterization, however, as apparent from Fig. 5, it entails a pretty relevant underestimation of losses (i.e. about 20% of the losses of the square profile at the same field and frequency). This confirms the relevance, in order to properly estimate the caloric performance of a material, of carrying measurements under excitation waveforms close to the ones expected in actual devices.

It is worth noting that the efficiency extrapolated from expression (2) takes into account, as a unique source of irreversibility, entropy production within the active material. All the other departures from a reversible Carnot cycle, either associated with the device design (i.e. non-isothermal heat ex-

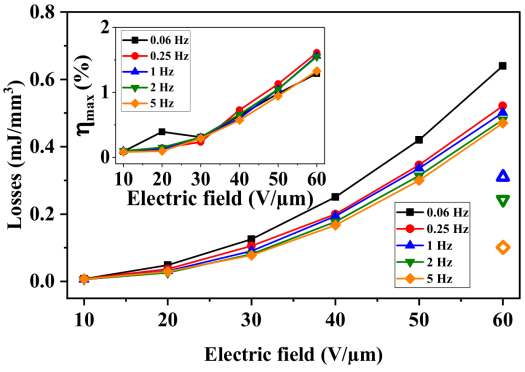

FIG. 5. Material losses as a function of the field measured at different frequencies. The open points show the losses measured under sinusoidal excitation with $E_{max} = 60$ Vμm^{-1} . Inset: maximum relative efficiency computed from Eq. 3

change, viscous losses associated with the moving parts [22] etc.) are neglected. From this standpoint, the efficiencies extrapolated here represent an upper bound for the overall efficiency of a cooling device deploying the considered material. The loss factor R has been extrapolated from the data shown in Fig. 4 and 5, assuming $T\Delta s \approx c_E \Delta T_{ad}$, where c_E is the specific heat at constant electric field of the electrocaloric film. The maximum relative efficiency η_{max} of a device using the EC polymer characterized here has been calculated and plotted in the inset of Fig. 5, getting to a maximum of $\approx 2\%$ for $E_{max} = 60\ \mathrm{V}\mu\mathrm{m}^{-1}$. Considering the rather good ΔT_{adia} shown by the studied terPo, the poor relative efficiency point at material loss as a major pitfall for using the material in cooling applications. Several issues are at stake in order to find strategies to reduce losses. Increasing the field always entails an improvement of the efficiency; however, most materials can not endure a field above $60\ \mathrm{V}\mu\mathrm{m}^{-1}$ without a relevant risk of breakdown. In addition, the operating frequency, and the excitation waveform are both key features affecting the losses. For instance, the measurements presented here show voltage steps taking place over a time of the order of 5% of the period; other experiments working with higher rates may lead to a slight increase of the losses. Considering that the relative efficiencies reported for some of the most promising devices using terPo refrigerants[4, 8] are parabolic with respect to ΔT_{res}, as predicted by Eq. (2), as a check of our approach, we used the reported [4, 8] ΔT_{adia}, jointly with the loss measured on the terPo studied here, for extrapolating the maximum relative efficiency from Eq.(2). The efficiencies reported in the literature are 6.1%[4] and 4%[8], the ones extrapolated here are 5.3% and 3.7%. Such a good agreement, also considering that it relies on the loss measured on our terPo samples, stresses that both devices are working close to the efficiency upper bound imposed by the material. This result is validating the method proposed here as a reliable tool to identify the leading mechanism responsible for the efficiency reduction of a given device. In the two cases studied here it shows that both devices are working close to the efficiency upper bound imposed by the material. To put it another way, as both devices are working close to the maximum efficiency, improvements have to be searched rather by reducing material losses, than by further optimization of the device design. The approach can be used to optimize new materials, focusing on both the caloric response, and the losses. The R figure of merit can help to set quantitative objectives to material studies: for instance, to achieve a relative efficiency above 50% the loss factor needs to be kept below 0.25 entailing a loss reduction by a factor 20. Interestingly, recent works on nanocomposites [13, 23] or especially on carbon double bound [15, 24] show a promising perspective, not only in terms of better ΔT_{ad} at low field but also of material loss reduction.

To summarize, although the traditional figure of merit in caloric cooling focuses on the amplitude and width of the $\Delta T_{ad}(T)$, we show that a novel figure of merit, taking into account material losses can pave the way to a more effective optimization of EC materials for a new generation of more efficient solid state based cooling devices.

This work has benefited from the financial support of the LabEx LaSIPS (ANR-10-LABX-0032-LaSIPS) under the "Investissements d'avenir" program (ANR-11-IDEX-0003) and from (ANR-20-CE05-0044), which are both managed by the French National Research Agency.

[1] B. Grocholski, "Cooling in a warming world," (2020).
[2] X. Moya and N. D. Mathur, Science **803**, 797 (2020).
[3] T. Correia and Qi Zhang, *Engineering Materials*, Vol. 34 (Springer, 2014) pp. 147–182.
[4] R. Ma, Z. Zhang, K. Tong, D. Huber, R. Kornbluh, Y. S. Ju, and Q. Pei, Science **357**, 1130 (2017).
[5] X. Moya, S. Kar-Narayan, and N. D. Mathur, Nature Materials **13**, 439 (2014).
[6] X. Moya, E. Defay, V. Heine, and N. D. Mathur, Nature Physics **11**, 202 (2015).
[7] M. Valant, Progress in Materials Science **57**, 980 (2012).
[8] Y. Meng, Z. Zhang, H. Wu, R. Wu, J. Wu, H. Wang, and Q. Pei, Nature Energy **5**, 996 (2020).
[9] Y. Liu, J. F. Scott, and B. Dkhil, Applied Physics Reviews **3** (2016), 10.1063/1.4958327.
[10] H. Callen, *Thermodynamics and an Introduction to Thermostatistics* (Wiley, 1985).
[11] S. G. Lu, B. Rožič, Q. M. Zhang, Z. Kutnjak, R. Pirc, M. Lin, X. Li, and L. Gorny, Applied Physics Letters **97**, 3 (2010).
[12] M. Bratko, K. Morrison, A. de Campos, S. Gama, L. F. Cohen, and K. G. Sandeman, Applied Physics Letters **100**, 252409 (2012).
[13] J. Qian, R. Peng, Z. Shen, J. Jiang, F. Xue, T. Yang, L. Chen, and Y. Shen, Advanced Materials **31**, 1 (2019).
[14] V. Basso, F. Russo, J. F. Gerard, and S. Pruvost, Applied Physics Letters **103** (2013), 10.1063/1.4830369.
[15] X. Qian, D. Han, L. Zheng, J. Chen, M. Tyagi, Q. Li, F. Du, S. Zheng, X. Huang, S. Zhang, J. Shi, H. Huang, X. Shi, J. Chen, H. Qin, J. Bernholc, X. Chen, L. Q. Chen, L. Hong, and Q. M. Zhang, Nature **600**, 664 (2021).
[16] W. Sabuga and R. Todtenhaupt, High Temperatures - High Pressures **33**, 261 (2001).
[17] G. G. Guzmán-Verri and P. B. Littlewood, APL Materials **4**, 064106 (2016).
[18] E. Defay, S. Crossley, S. Kar-Narayan, X. Moya, and N. D. Mathur, Advanced Materials **25**, 3337 (2013).
[19] S. Qian, D. Nasuta, A. Rhoads, Y. Wang, Y. Geng, Y. Hwang, R. Radermacher, and I. Takeuchi, International journal of refrigeration **62**, 177 (2016).
[20] G. Suchaneck, O. Pakhomov, and G. Gerlach, in *Refrigeration* (IntechOpen, 2017).
[21] H. S. Leff and G. L. Jones, American Journal of Physics **43**, 973 (1975).
[22] L. Depreux, M. Almanza, N. Zeggai, F. Parrain, and M. LoBue, Applied Thermal Engineering **211**, 118290 (2022).
[23] Y. Chen, J. Qian, J. Yu, M. Guo, Q. Zhang, J. Jiang, Z. Shen, L. Q. Chen, and Y. Shen, Advanced Materials **32**, 1 (2020).
[24] F. L. Goupil, K. Kallitsis, S. Tencé-girault, C. Brochon, E. Cloutet, T. Soulestin, D. Santos, N. Stingelin, G. Hadzioannou, F. L. Goupil, K. Kallitsis, S. Tencé-girault, N. Pouriamanesh, and C. Brochon, Advanced Functional Materials **31**, 2007043 (2020).